Climate response associated with the Southern Annular Mode in the surroundings of Antarctic Peninsula: A multimodel ensemble analysis

Andrea F. Carril,[1] Claudio G. Menéndez,[2] and Antonio Navarra[1]

Received 25 May 2005; revised 15 July 2005; accepted 3 August 2005; published XX Month 2005.

[1] This paper is an attempt to extract an average picture of the response of the Southern Annular Mode (SAM) to increasing greenhouse gases (GHG) forcing from a multimodel ensemble of simulations conducted in the framework of the IPCC 4th assessment experiments. Our analysis confirms that the climate change signal in the mid- to high southern latitudes projects strongly into the positive phase (PP) of the SAM. Over the present climate time slice (1970–1999), multimodel ensemble mean reproduce the regional warming around the Antarctic Peninsula (AP) associated with the SAM. When increasing GHG (future time slice, 2070–2099), warming in the neighborhoods of the AP and decreasing sea-ice volume in the sea-ice edge region in the Amundsen and Weddell Seas intensifies, suggesting that recent observed sea-ice trends around AP could be associated to anthropogenic forcings. Changes in surface temperature and sea-ice are consistent with anomalous atmospheric heat transport associated with circulation anomalies. **Citation:** Carril, A. F., C. G. Menéndez, and A. Navarra (2005), Climate response associated with the Southern Annular Mode in the surroundings of Antarctic Peninsula: A multimodel ensemble analysis, *Geophys. Res. Lett.*, *32*, LXXXXX, doi:10.1029/2005GL023581.

1. Introduction

[2] The Southern Annular Mode (SAM) is the principal mode of variability of the atmospheric circulation in the SH extratropics [*Thompson and Wallace*, 2000]. Many 20th century simulations exhibit a trend in the SAM towards its positive phase (PP) with a strengthening of the circumpolar vortex and intensification of the circumpolar westerlies [*Fyfe et al.*, 1999; *Kushner et al.*, 2001; *Cai et al.*, 2003; *Rauthe et al.*, 2004; *Shindell and Schmidt*, 2004]. This trend, occasionally not significant in the simulations, is also revealed by Antarctic station observations [*Marshall*, 2003]. The trend in the SAM has been attributed to ozone depletion [*Thompson and Solomon*, 2002] and GHG increase [*Kushner et al.*, 2001], but natural forcings may have acted synergistically with anthropogenic forcing [*Hartmann et al.*, 2000].

[3] Over the second half of the 20th century, Antarctic Peninsula (AP) stations show a strong warming trend, while stations in other antarctic areas show no significant trend or slight cooling [*Comiso*, 2000]. The AP record and the opposite cooling over most of Antarctica is consistent with circulation changes associated with the trend in the SAM [*Thompson and Wallace*, 2000; *Schneider et al.*, 2004]. In addition, local air-sea-ice interaction may also affect [*Marshall and King*, 1998]. While most of the AOGCMs analyzed for the IPCC 3rd Assessment Report (TAR) were able to reproduce the large scale features of the atmospheric circulation [*McAvaney et al.*, 2001] and the evolution of the global mean surface temperature, they failed to capture the enhanced warming in the AP region [*Vaughan et al.*, 2003].

[4] The IPCC 4th Assessment Model Output provides simulations of the 20th century climate and diverse idealized climate change scenarios. Our purpose is to investigate whether the pattern of changes associated with the SAM PP over the Southern Ocean and Antarctic periphery is reinforced under enhanced GHG forcing, and what pattern, if any, develops over the AP. We only analyze simulations of the 20th century climate (namely 20C3M) and of the 21st century climate according to the Special Report on Emission Scenarios (SRES) A2. The 20C3M experiment is an anthropogenically forced experiment over the historical period (initialized from a point close to a pre-industrial control run), with a length of about 100–150 years, depending on every single model. The SRES A2 experiment starts at the end of the 20C3M run and covers a period of about 100-yr during which GHG increment following the A2 emission scenario.

2. Data and Methodology

[5] We analyze results from 7 models from 7 modeling centers: 1) CNRM-CM3 (Météo-France, Centre National de Recherches Météorologiques, France), 2) GFDL-CM2.0 (NOAA, Geophysical Fluid Dynamics Laboratory, USA), 3) GISS-ER (Goddard Institute for Space Studies, NASA, USA), 4) IPSL-CM4 (Institut Pierre Simon Laplace, France), 5) MIROC3.2 medres (Center for Climate System Research, National Institute for Environmental Studies and Frontier Research Center for Global Change, Japan), 6) MRI-CGCM2.3.2 (Meteorological Research Institute, Japan), and 7) PCM (National Center for Atmospheric Research, NSF, DOE, NASA and NOOA, USA). Documentation of these models is available on the PCMDI web site (http://www-pcmdi.llnl.gov).

[6] Present and future climate is analyzed for periods of 30 years (1970–1999 and 2070–2099 respectively). The variables selected are monthly mean sea level pressure (SLP), surface temperature (TS), sea-ice concentration (SIC) and sea-ice volume (SIV). TS is the skin temperature and SIV is the sea-ice thickness (SIT) multiplied by the average area of the grid cell covered by sea-ice. For sea-ice

[1]Istituto Nazionale di Geofisica e Vulcanologia, Bologna, Italy.
[2]Centro de Investigaciones del Mar y la Atmósfera, Consejo de Investigaciones del Mar y la Atmosphere, Universidad de Buenos Aires, Buenos Aires, Argentina.

0094-8276/05/2005GL023581$05.00

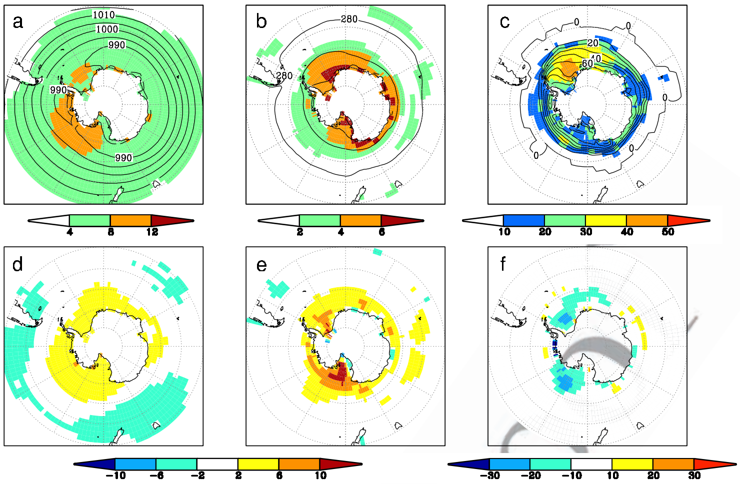

Figure 1. (a, d) Present climate (1970–1999) sea level pressure (SLP), (b, e) surface temperature (ST) and (c, f) sea-ice concentration (SIC). (top) The ensemble annual mean values (contours) and the inter-model standard deviation (shaded). (bottom) The difference between the present climate ensemble experiment and the reference climatology. Units are hPa for SLP, K for ST and [%] for SIC.

variables, the ensemble is done only by models 1, 3, 4, 5 and 6. Series for the analysis are linearly detrended; anomalies are relative to the best straight-line fit linear trend from the input data. Input data are annual mean but also seasonal mean series. NCEP dataset covering the period 1970–1999 is used to validate the simulation of SLP and TS, while the SIC is validated against the HadISST1.1 dataset [*Rayner et al.*, 2000] covering the period 1982–1999.

[7] The SAM is defined as the leading mode of the empirical orthogonal function (EOF-1) obtained from anomaly series of 500 hPa geopotential heights, area weighted by the square root of cosine of latitude. EOF domain is southern of 20°S. We identify events during which the PP of the SAM is particularly strong (events in which the principal component, PC-1, is above one standard deviation of its mean value). We perform composites of SLP, TS and SIV anomalies and examine the associated climate response.

3. Mean Present Climate and Response to Increasing GHG

[8] To summarize the performance of the models, we evaluate the annual mean (ANM) values of both the ensemble mean (the average over all the simulations) and the inter-simulation standard deviation (IMSD). While earlier models exhibit striking difficulties in simulating both the position and depth of the Antarctic trough, the new generation of AOGCMs seems to evince a better agreement with the NCEP reanalysis, with errors lower than 2 hPa over large areas of the Southern Ocean (Figures 1a and 1d). In comparison with CMIP2 results (Report 66 at www-pcmdi.llnl.gov), errors over large areas of Antarctic seas were reduced from 6–10 to 2–6 hPa. Because spurious large departures and IMSD occur over the high terrain area (due to the extrapolation below ground), a land-sea mask was applied. The ensemble mean tends to underestimate the SLP over the mid-latitudes and consequently the meridional gradient is relatively weak.

[9] The errors in model-mean TS (Figures 1b and 1e) are generally in the range of 2–6 K over most of the Southern Ocean. Errors are largest over the Ross Sea and relatively large over western Antarctic seas. However, the consensus among models is relatively high in the Amundsen-Bellingshausen seas. The sea-ice concentration ensemble-mean values are in rough accord with the observational dataset (Figures 1c and 1f). As in CMIP [*Covey et al.*, 2003] models tend, on average, to produce too little sea ice cover. But the biases rarely exceed 20% over most of the sub-Antarctic seas and it is just 30% in the eastern Ross Sea and in the Weddell Sea (regions where the across-model scatter is large). However, the opposite behavior is found along sectors of the sea-ice edge where the sea-ice extent is slightly overestimated.

[10] As in previous analyses [e.g., *Fyfe et al.*, 1999; *Kushner et al.*, 2001], then mean response to the anthropogenic forcing is a SAM-like pattern (Figure 2a). Moreover, in a warmer climate, the SAM PP (or a high index polarity) will be favored, leading to lower pressure over the Antarctic polar cap region and higher pressure over the mid-latitudes. It is an equivalent barotropic pattern and implies stronger westerly winds in the high latitudes.

[11] The ST response to increasing GHG (Figure 2b) exhibits a moderate warming in the southern mid- to high latitudes. The maximum warming is located in the Amundsen and Weddell seas. The SIC response (Figure 2c) exhibits a general decrease around Antarctica, maximum in the Amundsen-Bellingshausen Seas and in the eastern Weddell Sea. In contrast, weaker changes in ST are simulated along the coasts of eastern Antarctica and in general, around 55°–65°S, warming usually attributed to the large heat oceanic uptake due to the large deep ocean mixing (Figure 2b).

4. SAM-Related Variability

[12] In a warmer climate a modified meridional temperature gradient could alter wave propagation and

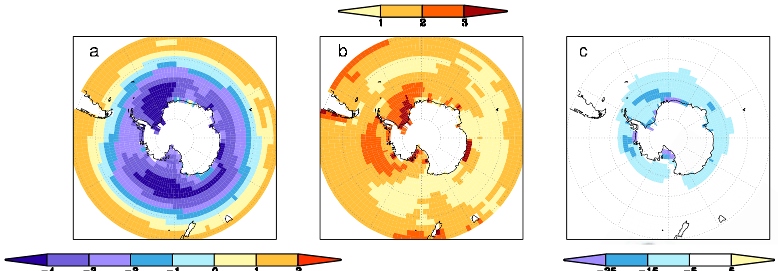

Figure 2. Projections of climate change as the annual mean differences between the SRES A2 experiment (2070–2099) and the present climate experiment (1970–1999); (a) SLP [hPa], (b) ST [K] and (c) SIC [%].

the westerly flow throughout the depth of the atmosphere. Therefore, the variability associated with the SAM could eventually alter its geographical pattern or structure. Hereafter, we explore into the potential climate variations associated with changes in the SAM PP, under enhanced GHG forcing. We focus on the austral late-spring season (OND) when the SAM is particularly strong.

[13] The general pattern of the composites of SLP anomalies (Figure 3, left) is essentially zonal with some anomalies superimposed particularly in the western Pacific sector. This pattern is similar for both periods, but for the later period both positive and negative anomalies are in general stronger. In other regions (southern Atlantic and Indian oceans) the changes are weaker and not uniform.

[14] The strong circumpolar flow along 60°S associated with the PP of the SAM tends to isolate the cold Antarctic region from warmer air in the lower latitudes which leads in general to cooler temperatures around the continent (Figure 3, middle). An exception is the Bellingshausen Sea-AP region, where anomalous strong meridional winds lead to increase warm advection from the north. Under enhanced GHG forcing (2070–2099), anomalies intensify and a dipole pattern between the AP region and large areas in the Weddell Sea (especially its eastern and northern sectors) is visible.

[15] Both observational [*Liu et al.*, 2004] and numerical [*Hall and Visbeck*, 2002] studies have found connections between the SAM and the sea-ice variability. We focus on the SIV (instead of the SIC) since this quantity integrates the 3-dimentional variability of the sea-ice in the models. The SIV composites associated with the PP of the SAM in the present-day period (Figure 3, right) show negative anomalies along the eastern coast of the Antarctica Peninsula and over the edge region in the Bellingshausen/Amundsen Seas, and positive anomalies in the Ross Sea region. This qualitatively agrees with the recently documented observational relationship between SAM and sea-ice [*Liu et al.*, 2004]. In a warmer climate, positive ST anomalies in the surroundings of the AP are related to negative anomalies in SIV over the edge region in Amundsen and Weddell Seas, and over the east coast of the AP. On the contrary, positive SIV anomalies are projected in vast areas over the Ross Sea and in the central Weddell Sea. The strong equatorward (poleward) flux at the surface promotes (confines) sea ice expansion.

[16] The sea ice variability is forced by a combination of both thermodynamic and dynamic processes that are

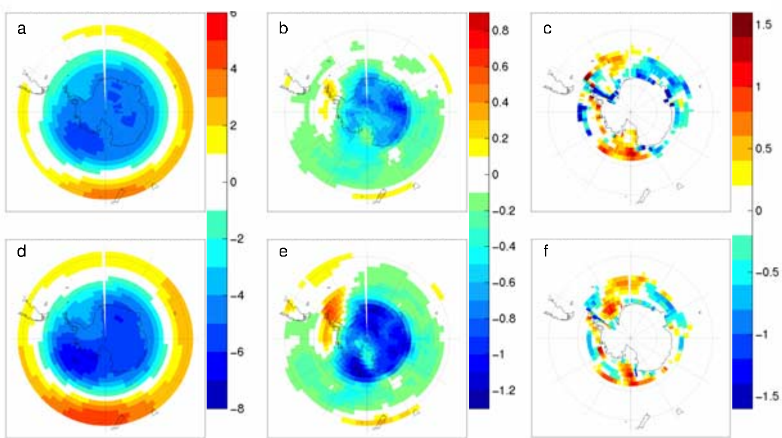

Figure 3. Composite anomalies of (a, d) SLP, (b, e) TS and (c, f) SIV for the SAM positive phase (PP). (top) The present climate experiment and (bottom) the climate change experiment. Season is OND. Units are hPa for SLP, K for ST and m^3 for SIV.

consistent with the atmospheric conditions. *Liu et al.* [2004] suggest a mechanism to explain the observed pattern of ice anomalies associated with the PP of the SAM, which could be pertinent for explaining the simulated SIV increase in the Ross and eastern Weddell seas (especially for the 2nd time slice). The intensification of the surface westerlies induces an enhanced Ekman drift to the north, which transports cold water, reducing the oceanic poleward heat transport. The associated enhanced northward ice advection decreases ice thickness and provides more open water for new ice formation. The newly formed ice is then advected to the north increasing ice concentration and thickness. On the contrary, the maximum warming and SIV decrease in the edge in Amundsen and western Weddell Seas associated with the positive SAM index likely occurs due to the strong anomalous poleward surface heat flux over a region of ice divergence. *Hall and Visbeck* [2002] propound similar mechanisms related to the influence of the SAM on the ocean and ice conditions in a long simulation performed with a low resolution coupled model. Finally, positive SIV anomalies along the western coast of the AP could be related with a mechanical effect of sea-ice accumulation over physical barrier.

5. Final Remarks

[17] We have documented the relationship between the SAM and surface features of the regional climate around Antarctica through the analysis of simulations from a multimodel ensemble in the framework of the IPCC AR4. We describe the variability in two 30-year time slices (1970–1999 and 2070–2099), with emphasis in the region around the AP, during the austral late spring. The SLP pattern of anomalies associated with the SAM PP enhances the westerly winds at 60°S especially in the Pacific Ocean and promotes strong anomalous surface heat fluxes. During both periods, the anomalies in temperature advection cause a warming in the AP region but a general cooling around the rest of Antarctica. In general, these patterns are reinforced during the second time slice. The confidence in sea-ice anomalies response is limited by the reduced number of models providing sea-ice information and the large inter-model standard deviation. Nevertheless, sea-ice anomalies associated with the SAM resemble the observed changes in the Antarctic SIC associated with the SAM index [*Liu et al.*, 2004], suggesting that the models are simulating to some extent realistic variability.

[18] When individual model simulations are analyzed, a consensus about the intensification of the SAM pattern in a warmer climate is reached during the austral spring and summer (but not during the fall and winter); while SAM dominates the climate change signal in annual mean conditions. On the other hand, the linear amplification of the warming around the AP when increasing GHG is a characteristic that dominate during the late spring. In summer, other mechanisms might be interacting, and the climate response to the intensification of the SAM is more complex. Moreover, decadal fluctuations in the climate system could be modulating the SAM and the SAM-related signal; then variability from longer time slices could be comparatively weaker.

[19] Even if the large-scale circulation changes associated with the SAM are important drivers of the AP climate change, its regional expression is likely to be strongly controlled by local interactions between atmosphere, ocean and sea-ice. Furthermore, the SAM response is transient and, possibly once CO_2 concentration stabilizes, the upward SAM trend could reverse [*Cai et al.*, 2003]. If the stratospheric ozone recovery -which is expected over the coming decades- is taking into account, the SAM variability could also be affected [*Shindell and Schmidt*, 2004]. Consequently we emphasize that the results need to be viewed with caution, given the weaknesses in the models and the uncertainties related to the future transient evolution of GHG and ozone forcings.

[20] **Acknowledgments.** We acknowledge the international modeling groups for providing their data for analysis, the Program for Climate Model Diagnosis and Intercomparison (PCMDI) for collecting and archiving the model data, the JSC/CLIVAR Working Group on Coupled Modelling (WGCM) and their Coupled Model Intercomparison Project (CMIP) and Climate Simulation Panel for organizing the model data analysis activity, and the IPCC WG1 TSU for technical support. The IPCC Data Archive at Lawrence Livermore National Laboratory is supported by the Office of Science, U.S. Department of Energy. This research was done in the framework of CLARIS EU project. A. F. Carril was partially supported by CLARIS (GOCE-CT-2003-01454) and by MERSEA IP project (SIP3-CT-2003-502885) and C.G. Menéndez by CONICET (Argentina).

References

Cai, W., P. H. Whetton, and D. J. Karoly (2003), The response of the Antarctic Oscillation to increasing and stabilized atmospheric CO_2, *J. Clim.*, *16*, 1525–1538.

Comiso, J. C. (2000), Variability and trends in Antarctic surface temperatures from in situ and satellite infrared measurements, *J. Clim.*, *13*, 1674–1696.

Covey, C., K. M. AchutaRao, U. Cubasch, P. Jones, S. J. Lambert, M. E. Mann, T. J. Phillips, and K. E. Taylor (2003), An overview of results from the Coupled Model Intercomparison Project (CMIP), *Global Planet. Change*, *37*, 103–133, doi:10.1016/S0921-8181(02)00193-5.

Fyfe, J. C., G. J. Boer, and G. M. Flato (1999), The Arctic and Antarctic Oscillations and their projected changes under global warming, *Geophys. Res. Lett.*, *26*, 1601–1604.

Hall, A., and M. Visbeck (2002), Synchronous variability in the Southern Hemisphere atmosphere, sea ice, and ocean resulting from the annular mode, *J. Clim.*, *15*, 3043–3057.

Hartmann, D. L., J. M. Wallace, V. Limpasuvan, D. W. J. Thompson, and J. R. Holton (2000), Can ozone depletion and global warming interact to produce rapid climate change?, *Proc. Natl. Acad. Sci. U.S.A.*, *97*, 1412–1417.

Kushner, P. J., I. M. Held, and T. L. Delworth (2001), Southern Hemisphere atmospheric circulation response to global warming, *J. Clim.*, *14*, 2238–2249.

Liu, J., J. A. Curry, and D. G. Martinson (2004), Interpretation of recent Antarctic sea ice variability, *Geophys. Res. Lett.*, *31*, L02205, doi:10.1029/2003GL018732.

Marshall, G. J. (2003), Trends in the Southern Annular Mode from observations and reanalyses, *J. Clim.*, *16*, 4134–4143.

Marshall, G. J., and J. C. King (1998), Southern Hemisphere circulation anomalies associated with extreme Antarctic Peninsula winter temperatures, *Geophys. Res. Lett*, *25*, 2437–2440.

McAvaney, B. J., et al. (2001), Model evaluation, in Climate Change 2001: The Scientific Basis: Contribution of Working Group I to the Third Assessment Report of the Intergovernmental Panel on Climate Change, edited by J. T. Houghton et al., pp. 471–523, Cambridge Univ. Press, New York.

Rauthe, M., A. Hense, and H. Paeth (2004), A model intercomparison study of climate change signals in extratropical circulation, *Int. J. Climatol.*, *24*, 643–662.

Rayner, N. A., D. E. Parker, P. Frich, E. B. Horton, C. K. Folland, and L. V. Alexander (2000), The HadISST1 Global Sea-Ice and Sea Surface Temperature Dataset, 1871–1999, *Clim. Res. Tech. Note 17*, Met Off. Hadley Cent., Bracknell, UK.

Schneider, D. P., E. J. Steig, and J. C. Comiso (2004), Recent climate variability in Antarctica from satellite-derived temperature data, *J. Clim.*, *17*, 1569–1583.

Shindell, D. T., and G. A. Schmidt (2004), Southern Hemisphere climate response to ozone changes and greenhouse gas increases, *Geophys. Res. Lett.*, *31*, L18209, doi:10.1029/2004GL020724.

Thompson, D. W., and S. Solomon (2002), Interpretation of recent Southern Hemisphere climate change, *Science*, *296*, 895–899.

Thompson, D. W. J., and J. M. Wallace (2000), Annular modes in the extratropical circulation, part I: Month-to-month variability, *J. Clim.*, *13*, 1000–1016.

Vaughan, D. G., G. J. Marshall, W. M. Connolley, C. Parkinson, R. Mulvaney, D. A. Hodgson, J. C. King, C. J. Pudsey, and J. Turner (2003), Recent rapid regional climate warming on the Antarctic Peninsula, *Clim. Change*, *60*, 243–274.

A. F. Carril and A. Navarra, National Institute of Geophysics and Volcanology, Via Donato Creti 12, I-40128 Bologna, Italy. (carril@bo.ingv.it; navarra@bo.ingv.it)

C. G. Menéndez, Centro de Investigaciones del Mar y la Atmósfera, Pabellón 2 Piso 2, Ciudad Universitaria, 1428, Buenos Aires, Argentina. (menendez@cima.fcen.uba.ar)